



# A new predictor parameter for production rate of ornamental stones

Amin Jamshidi<sup>1</sup>

Received: 16 October 2017 / Accepted: 5 March 2018 / Published online: 13 March 2018  
© Springer-Verlag GmbH Germany, part of Springer Nature 2018

## Abstract

In this study, a new predictor parameter (NPP), which is based on the product of uniaxial compressive strength (UCS) and Mohs hardness (MH), was proposed for prediction of production rate (PR) of ornamental stones. For this, the PR, MH and UCS of ten different igneous stones were determined, and then their NPP was calculated. Using data analysis, a statistical equation has been developed between PR and NPP using simple regression analysis. The validity of NPP for prediction of PR was investigated using the raw data obtained from experimental works of two researchers. It was concluded that the NPP has good accuracy for prediction of PR, and thus making a rapid PR assessment of stones. As a result, the NPP proposed in this study provides significant practical advantages in predicting the cost and production schedule.

**Keywords** Mohs hardness · Ornamental stones · Predictor parameter · Production rate · Uniaxial compressive strength

## Introduction

Circular diamond saws have been widely used in stone processing plants. These saws are successfully used because they cut fast, are flexible and economical, and are easy to operate at a good accuracy on the cut surface (Ersoy and Atici 2004). Stone sawability is affected by the complex interaction of many effective parameters that are classified in three major categories as follows (Mikaeil et al. 2013a):

- Stone characteristics
- Sawing and operational characterization of machine
- Operating skills and working conditions

Among them, the sawing characteristics and the operating skills could be controlled in the sawing process, but the stone characteristics are not controllable.

Stone sawability can be measured in terms of the production rate (PR). PR, which is also referred to as slab production or cutting rate, is the quantity of the area cut per unit time and generally expressed as  $\text{cm}^2/$

s or  $\text{m}^2/\text{h}$ . PR in practice can be calculated from the following equation,

$$\text{PR} = (L \times H)/t$$

where PR is production rate ( $\text{m}^2/\text{h}$ ), L is the stone block length (m), H is the stone block height (m) and t is the cutting time (h).

The stone PR is one of the most significant factors that have an effect on either the machine selection procedure or machine performance. Machine performance in its own turn, has a direct impact on production planning and cost estimation (Tumac 2015). Hence, the correct prediction of stone PR using inexpensive and simple methods became very important in the stone processing industry for a low-cost production and optimum cutting machine operation.

Till now, various researchers studied the relationship between sawability and stone characteristics in stone processing. The most important of them are given in Table 1.

Norling (1971) investigated the relationship between sawability and petrographic characteristics and concluded that grain size was more relevant to sawability than the quartz content. Burgess (1978) developed a statistical model for sawability, which was based on hardness, abrasion resistance, mineralogical composition and grain size. Gunaydin et al. (2004) investigated the relationships between sawability and different brittleness indexes using regression analysis. They concluded that sawability of carbonate rocks

✉ Amin Jamshidi  
Jamshidi.geo85@yahoo.com

<sup>1</sup> Department of Geology, Lorestan University, Khorramabad, Iran

**Table 1** Part of the previous research on the relationship between PR and stone characteristics

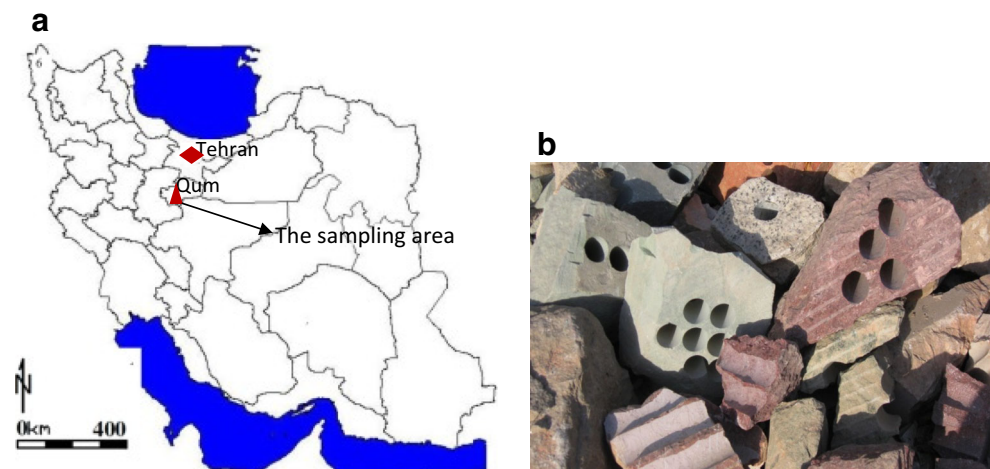
Researcher/s	Investigated stone characteristics											
	UCS	BTS	YM	IS	C	H	A	D	P	GS	QC	B
Burgess (1978)										×	×	
Wright and Cassapi (1985)	×	×				×	×				×	
Jennings and Wright (1989)	×	×				×					×	
Clausen et al. (1996)										×	×	
Eyuboglu et al. (2003)	×	×	×			×						
Kahraman et al. (2004)	×	×		×		×	×					
Gunaydin et al. (2004)	×	×		×								×
Ozcelik et al. (2004)	×	×	×			×		×			×	
Ersoy et al. (2005)	×	×	×	×			×	×			×	
Delgado et al. (2005)						×					×	
Kahraman et al. (2006)					×				×			
Fener et al. (2007)	×	×		×		×	×					
Ozcelik (2007)	×	×				×					×	
Buyuksagis (2007)	×	×				×	×	×			×	
Mikaeil et al. (2008)	×										×	
Atici and Ersoy (2009)	×	×										
Guney (2011)						×				×		
Mikaeil et al. (2013a)												×
Mikaeil et al. (2013b)	×		×			×						
Ghaysari et al. (2012)										×		
Tumac (2015)	×	×				×	×					
Tumac (2016)	×	×										
Almasi et al. (2017a)	×					×				×		

UCS uniaxial compressive strength, YM Young's modulus, BTS Brazilian tensile strength, IS impact strength, C cohesion, H hardness, A abrasivity, D density, P porosity, GS grain size, QC quartz content, B brittleness index

can be estimated from the rock brittleness. Delgado et al. (2005) experimentally studied the relationship between the sawability of granite and its micro hardness. Their results indicated that the use of the Vickers hardness microindenter

could provide more reliable information in sawability studies. Mikaeil et al. (2008) estimated the sawability of diamond wire cutting in carbonate rocks. They investigated the relationship between production rate and rock characteristics (equivalent

**Fig. 1** a) The sampling area on a map of Iran b) some of the stone blocks for laboratory tests



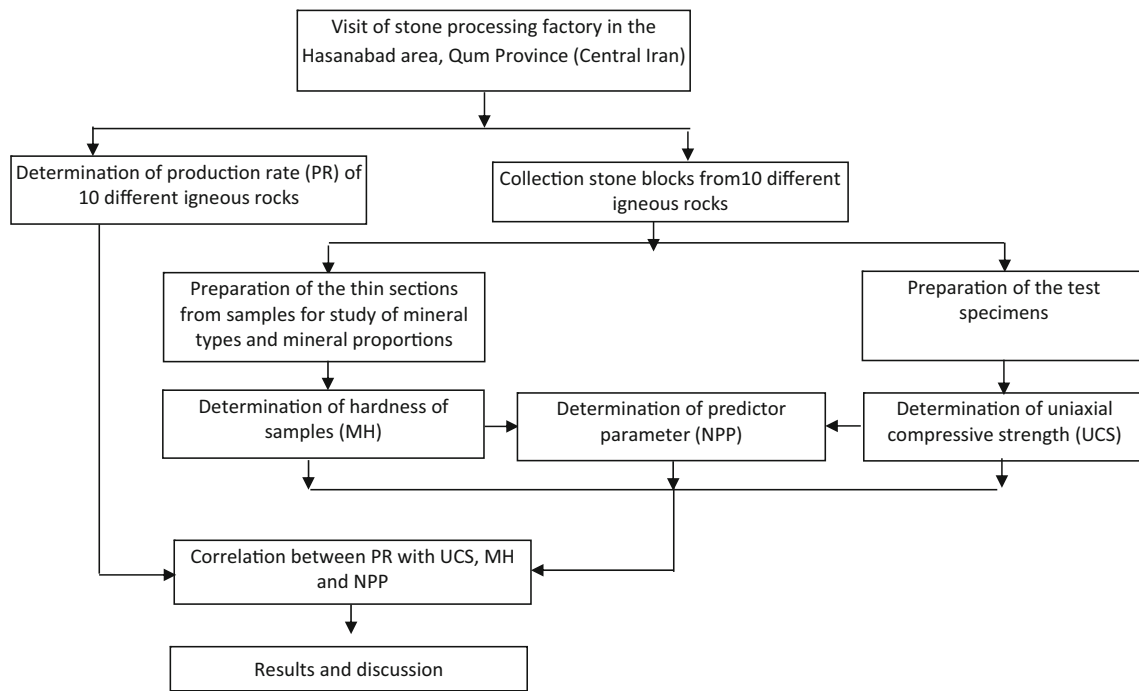


Fig. 2 Methodology of the research

quartz content and uniaxial compressive strength) using multiple curvilinear regression analysis. Ataei et al. (2012) predicted the production rate of a diamond wire saw based on rock characteristics, using statistical regression analysis. Mikaeil et al. (2013a) used rock brittleness as a predictor to estimate the production rate of ornamental stones using simple regression analysis. They showed that there is not a good relationship between the production rate and  $B_1$  (the ratio of compressive strength to tensile strength) and  $B_2$  (the ratio of compressive strength minus tensile strength to compressive strength plus tensile strength). However, there is a reliable prediction for production rate based on  $B_3$  (half of the product of compressive strength and tensile strength) as a brittleness index. Almasi et al. (2017a) investigated relationships between production rate and rock characteristics for eleven types of hard dimension stones. These researchers found out that the Mohs hardness, uniaxial compressive strength and grain size are the most important parameters for rock sawability prediction.

As can be seen from the literature review, there are several studies related to predicting the sawability from rock characteristics. In recent years, researchers have been attracted to new approaches for solution of natural stones problems such as sawability of building stones. These methods are based on genetic algorithms, support vector regression (Beiki et al. 2013; Ceryan 2014), probabilistic and soft computing techniques, such as artificial neural networks, regression trees (Bianconi et al. 2012; Yurdakul et al. 2014; Aydin et al. 2015; Armaghani et al. 2016; Tumac 2016; Singh et al.

2017), adaptive neuro-fuzzy inference systems, fuzzy inference systems, a hybrid ANN and GA, hybrid ANN and imperialist competitive algorithms, and the hybrid ANN and particle swarm optimization technique (Monjezi et al. 2012; Mikaeil et al. 2013b; Mishra and Basu 2013; Kainthola et al. 2015; Mohamad et al. 2015; Madhubabu et al. 2016).

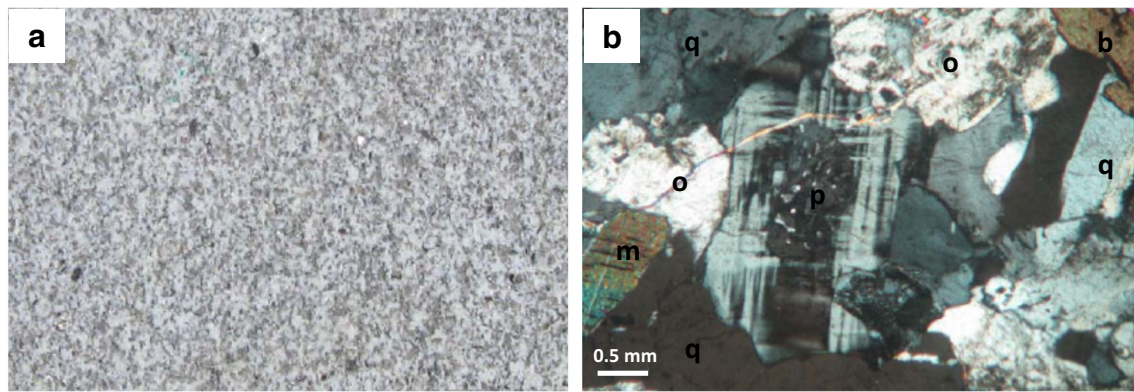
In this study, a new predictor parameter (NPP), which is based on product of uniaxial compressive strength (UCS) and Mohs hardness (MH), was proposed for prediction of production rate (PR) of ornamental stones. This approach can save a

Table 2 The production rate, uniaxial compressive strength, Mohs hardness and the predictor parameter of the samples under study

Scientific name	PR (m <sup>2</sup> /h)	UCS (MPa)	MH	*NPP (MPa)
Granite-I	5.7	98.1	5.12	502.27
Granite-II	6.4	80.5	5.36	431.48
Granite-III	5.0	121.0	6.12	740.52
Granite-IV	5.8	109.8	5.30	581.94
Granite-V	3.8	157.3	6.61	1039.75
Andesite-I	4.6	117.0	6.13	717.21
Andesite-II	6.6	96.5	5.01	483.47
Diorite	4.3	147.9	6.00	887.40
Rhyolite	4.9	130.3	5.70	742.71
Ignimbrite	6.4	94.7	5.28	500.02

PR production rate, UCS uniaxial compressive strength, MH Mohs hardness, NPP predictor parameter

\* The product of UCS and MH



**Fig. 3** a) Close-up and b) Polarizing microscopy images one of the studied stones (Granite-I) p, plagioclase; o, orthoclase; q, quartz; b, biotite; m, muscovite

lot of time and cost in the planning and design of the quarries and stone processing plants.

## Materials and methods

Stone processing factories in Hasanabad of Iran, Qum Province, were visited, and the production rate of diamond circular saws was recorded on ten different igneous rocks. These rock samples were selected due to their different mineralogical and mechanical characteristics and also different

resistance to cutting. Then, some samples of stone blocks were collected from the factories for laboratory studies. Each block sample was inspected for macroscopic defects so that it would provide test specimens free from fractures, partings or alteration zones (Gunaydin et al. 2004). Figures 1 and 2 show the location of factories and some samples of stone blocks. In the following, standard test specimens were prepared from these block samples and uniaxial compressive strength tests were performed. Test procedures were followed in accordance with suggested methods adopted by the International Society for Rock Mechanics (ISRM 1981). For petrographic

**Table 3** Type, class, mineralogical composition and textural properties of the stones under study

Rock type	Rock class	Mineralogical composition and textural properties
Granite-I	Igneous	Medium to coarse-grained and granular texture. Quartz, orthoclase and muscovite are the main minerals, plus a less amount of plagioclase and biotite. Orthoclase partly altered to sericite.
Granite-II	Igneous	Composed mainly of quartz, Alkali-feldspar (microcline) and muscovite. Plagioclase and biotite are minor. Most minerals not uniformly distributed. Granular texture.
Granite-III	Igneous	Subhedral to euhedral plagioclases and quartz. Biotite are seen as platy shapes and generally altered to sericite. Amphibole is less than 3%. Texture: granular.
Granite-IV	Igneous	Medium-grained and granular texture. Main minerals observed are feldspar, quartz, pyroxene and biotite. Pyroxene and biotite minerals are rich in cracks. Sericite formation can be seen in biotite.
Granite-V	Igneous	Coarse-grained and granular texture. Minerals: feldspar, quartz and biotite are the main minerals. Amphibole and pyroxene are seen as accessory minerals. Biotite is seen as platy shapes and generally altered.
Andesite-I	Igneous	Seriate texture, porphyritic glassy matrix. Main minerals observed are Alkali-feldspar and plagioclase that are more or less equidimensional. Matrix is generally made up of a high iron content.
Andesite-II	Igneous	Fine-grained, strongly bonded, very angular crystals and very tight grain boundaries. Texture is porphyritic composed mainly of quartz, and phenocrysts including pyroxene, feldspar, volcanic glass, etc.
Diorite	Igneous	Amphibole and plagioclase are the main minerals. Amphibole partly altered to chlorite. Garnet, sphene and epidotic can be observed in different dimensions.
Rhyolite	Igneous	Fine-grained texture. Fine grain quartz and Alkali-feldspar are within the vitreous groundmass. Less than 3% muscovite occur in the rock.
Ignimbrite	Igneous	Coarse-grained microcline phenocrysts and orthoclase and typically, red colored orthoclase is the predominant mineral, showing perthitic texture of anhedral quartz, subhedral to anhedral plagioclase, polysynthetic albite twinning and distinctively zoned subhedral plagioclase crystals (albite).

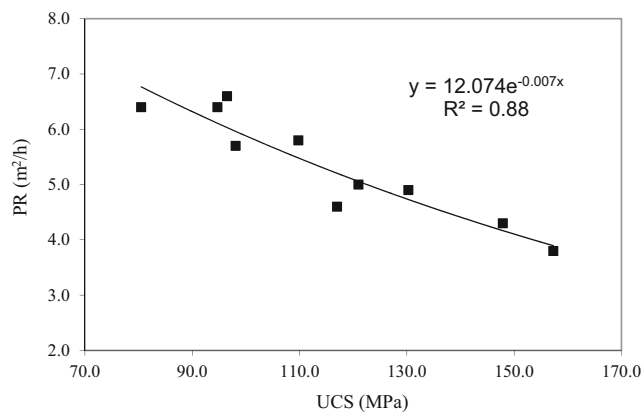


Fig. 4 The correlation between PR and UCS

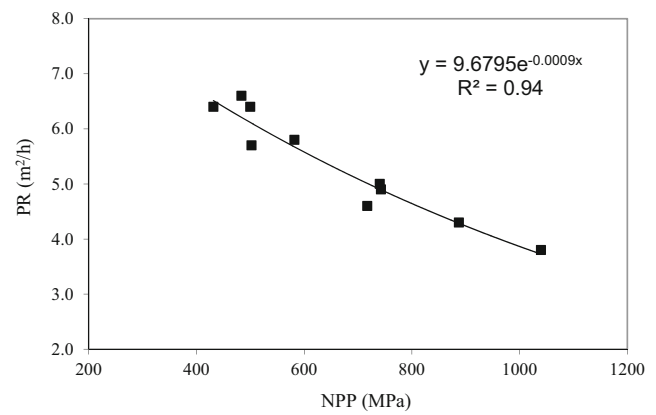


Fig. 6 The correlation between PR and NPP

characteristics including mineral types and mineral proportions, thin sections from each stone type were prepared. Based on these characteristics, the Mohs hardness of each stone type was determined. The NPP of stones was calculated from UCS and MH. Simple regression analyses were used in order to investigate the relationships between PR with UCS, MH and NPP. Based on regression analyses, the determination coefficients of relationships were determined. Finally, the validity of NPP for prediction of PR was investigated using the raw data obtained from experimental works of two researchers. Methodology of the research is given in Fig 2.

### New predictor parameter (NPP)

Linking the PR of building stones to their physical and mechanical characteristics, including strength, Young’s modulus, cohesion, hardness, abrasivity, density, porosity, grain size, and quartz content, has been a long-term aim which has generated great interest in many fields such as material science, mining engineering and engineering geology (Delgado et al. 2005; Ozcelik 2005; Mikaeil et al. 2008; Ataei et al. 2012;

Sadegheslam et al. 2013; Bagherpour et al. 2014; Almasi et al. 2017a, b).

The PR predictor is defined based on physical and mechanical characteristics of the stone. By applying the PR predictor, it saves much time and provides significant practical advantages for making a rapid PR assessment of stones and thus predicting the cost and production schedule. There are several studies related to predicting the PR from strength and hardness (Kahraman et al. 2004; Gunaydin et al. 2004; Kahraman et al. 2006; Mikaeil et al. 2013a; Tumac 2015, 2016; Almasi et al. 2017b). Results show that the PR of building stones decreases with increasing strength and hardness. In previous studies for predicting the PR, the strength and hardness have been used separately. However, the author of this study believes, when both the strength and hardness are taken into consideration with each other, the more accurate results for predicting the PR can be achieved. Thus, we propose a new predictor parameter (NPP) for predicting the PR of stones, which is based on the product of uniaxial compressive strength (UCS) and Mohs hardness (MH). The higher values of NPP indicate higher resistance of stone against production rate. The NPP is defined as follows:

$$NPP \text{ (MPa)} = UCS \times MH \tag{1}$$

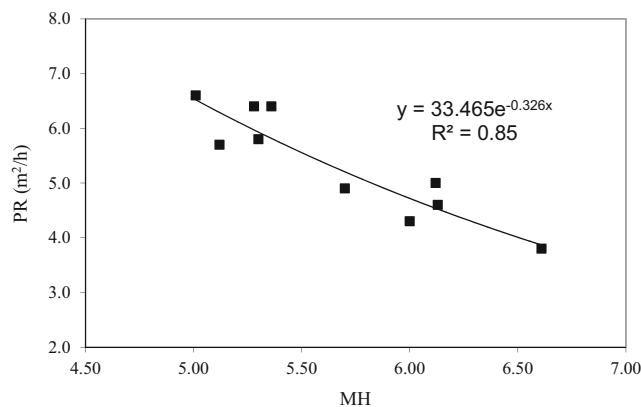


Fig. 5 The correlation between PR and MH

where UCS (MPa) and MH are the uniaxial compressive strength and Mohs hardness of stones, respectively.

The UCS test procedure was followed in accordance with ISRM (1981). For each stone type, the measurements were made on five specimens. These tests were conducted on core specimens with a diameter of 54.7 mm and a height-to-diameter ratio of approximately 2.5. The ends of the core specimens were flattened within 0.02 mm and were kept perpendicular within 0.05 mm so that loads could be applied uniformly. The stress rate was kept at 0.5 MPa/s. The mean values of UCS are listed in Table 2. Studied samples are also classified according to their UCS values as suggested in ISRM (2007). Using the tests results, the stones fall into the rocks

**Table 4** Summarizing the regression analyses results by t-test

Equation number	Regression equation	Determination coefficient ( $R^2$ )	t-value	
			Computed	Tabulated
3	$PR = 12.074 e^{-0.007UCS}$	0.88	-13.69	$\pm 2.262$
4	$PR = 33.465 e^{-0.326MH}$	0.85	-16.73	$\pm 2.262$
5	$PR = 9.6795 e^{-0.0009NPP}$	0.94	-10.47	$\pm 2.262$

class with high and medium strengths (50–100 MPa and 100–250 MPa, respectively).

Determination of petrographical characteristics not only provides information on the mineralogical composition and provenance of the rock origin, but also it is an important tool for assessing their mechanical characteristics and resistance against sawability. Here, thin sections obtained from stones were examined under an optical microscope to determine their petrographical characteristics (Fig. 3). A norm was used for determination of mineralogical composition of the vitreous part of some rocks such as andesite. A norm is essentially a set of idealized mineral-like components that are calculated from a bulk chemical analysis of a rock. For this reason, major element abundances were measured using a Rigaku ZSX100e X-Ray fluorescence spectrometer (XRF). Practically all norms were calculated by using a computer (Igpct software). Igpct software commonly has a section on calculating a CIPW Norm. In the Igpct software, we added the amount of all major elements and then calculated the CIPW normative compositions for the vitreous part of volcanic rocks. Type, class, mineralogical composition and textural properties of the samples are given in Table 3.

Hardness is the resistance of a mineral or rock against abrasion or scratching. Mohs hardness is defined for minerals generally. In this research, after determination of mineralogical composition and mineral proportions of the stones by thin sections studies, the mean hardness of each stone was calculated based

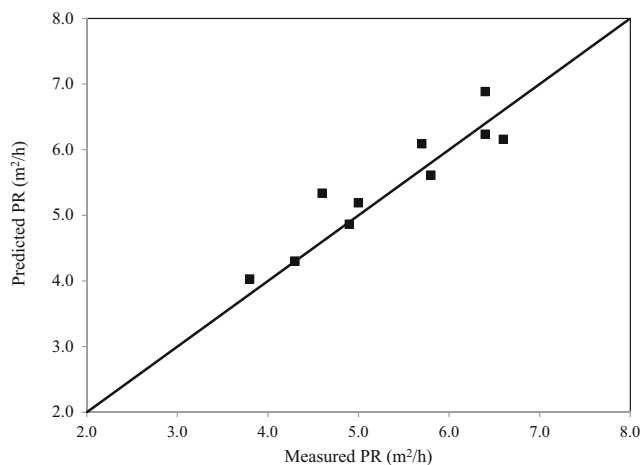
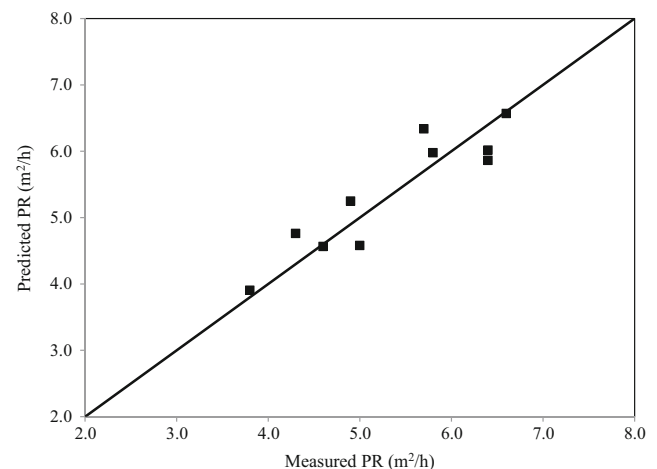
on hardness of the minerals contained using the following relation (Chatterjee et al. 2005):

$$\text{Hardness} = \sum_i^n A_i \times H_i \quad (2)$$

where A is the mineral proportion (%), H is Mohs hardness for each mineral type, and n is the number of minerals in rock. The results of these determinations are given in Table 2.

## Analysis of results

In order to investigate the relationships between PR with UCS, MH and NPP, linear ( $y = ax + b$ ), power ( $y = ax^b$ ), exponential ( $y = ae^x$ ) and logarithmic ( $y = a + \ln x$ ) regression analyses were, tried and the most reliable empirical equation with the highest determination coefficient was determined for each regression. The equation of the best-fit line, the 95% confidence level, and the determination coefficients ( $R^2$ ) were calculated for the above relationships. Figures 4, 5, and 6 show the relationships between PR with UCS, MH and NPP. There are exponential relationships between PR and UCS, and MH of the samples with determination coefficients of 0.88 and 0.85, respectively:

**Fig. 7** Measured PR versus predicted PR from Eq. 3**Fig. 8** Measured PR versus predicted PR from Eq. 4

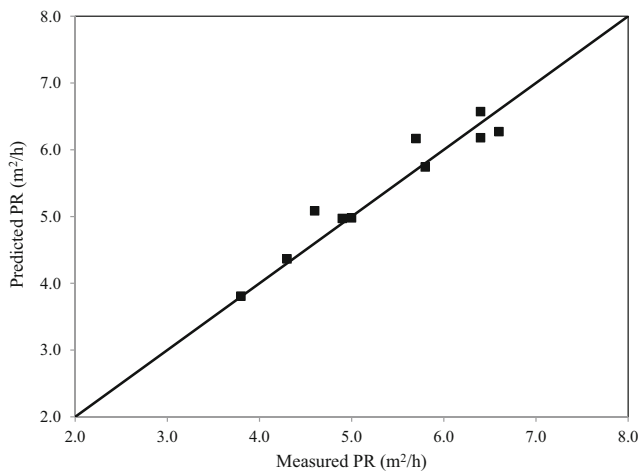


Fig. 9 Measured PR versus predicted PR from Eq. 5

$$PR = 12.074 e^{-0.007UCS} \quad R^2 = 0.88 \quad (3)$$

$$PR = 33.465 e^{-0.326MH} \quad R^2 = 0.85 \quad (4)$$

As seen from Figs. 4 and 5, PR is inversely related to UCS and MH. These results are in accordance with the findings of Gunaydin et al. (2004), Mikaeil et al. (2013a), Tumac (2015, 2016), Almasi et al. (2017a, b). Results of these researchers on the different rocks showed that the PR decreases with increasing UCS and MH.

A good exponential relationship was obtained between the PR and NPP with a determination coefficient of 0.94 according to the equation below:

$$PR = 9.6795 e^{-0.0009NPP} \quad R^2 = 0.94 \quad (5)$$

As seen from Fig. 6, the PR of samples decreases with increasing NPP. According to Eqs. 3–5, NPP showed stronger correlation with the PR ( $R^2 = 0.94$ ) when compared with the correlation between UCS and MH with PR ( $R^2 = 0.88$  and  $R^2 = 0.85$ , respectively).

The determination coefficients of the Eqs. 3–5 are 0.85, 0.88 and 0.94, respectively. These values are good, but they do not necessarily identify the valid Eqs. Therefore, other tests or methods must be performed. Validation of the Eqs. 3–5 was carried out by considering the t-test and the plots of predicted PR values versus the measured PR values. The statistical results of the three Eqs. are summarized in Table 4.

The significance of determination coefficients value can be evaluated by the t-test, assuming that both variables are normally distributed, and the observations are chosen randomly. The test compares the computed t-value with a tabulated t-value using the null hypothesis. In this study, a 95% level of confidence was chosen. If the computed t-value is greater than the tabulated t-value, the null hypothesis is rejected. This means that r is significant. If the computed t-value is less than the tabulated t-value, the null hypothesis is not rejected. In this case, r is not significant (Jamshidi et al. 2017). Since a 95% confidence level was chosen in this test, a corresponding critical t-value  $\pm 2.262$  is obtained from the related tables for Eqs. 3–5. It can be seen from Table 4 that all the computed t-values are greater than the tabulated t-values. This indicates that the equations are statistically meaningful and can be used for prediction of PR from UCS, MH and NPP.

To study the prediction capability of the Eqs. 3–5, the scatter diagrams of the predicted and measured values was employed. The plots of predicted versus measured values of PR for the equations are illustrated in Figs. 7, 8, and 9. The error in the predicted value is

**Table 5** The values of PR, UCS and MH from the Mikaeil et al. (2013b) research and also their calculated values of NPP from Eq. (1) developed in this study

Commercial name	Scientific name	Rock class	PR (m <sup>2</sup> /h)	UCS (MPa)	MH	NPP (MPa)
Harsin marble	Marble	Metamorphic	8.5	71.5	3.50	250.25
Anarak marble	Marble	Metamorphic	9.0	74.5	3.20	238.40
Azarshahr travertine	Travertine	Sedimentary	11.0	53.0	2.90	153.70
Hajiabad travertine	Travertine	Sedimentary	10.0	61.5	2.90	178.35
Darebokhari travertine	Travertine	Sedimentary	10.0	63.0	2.95	185.85
Salsali marble	Marble	Metamorphic	9.0	68.0	3.10	210.80
Haftoman marble	Marble	Metamorphic	8.0	74.5	3.60	268.20

PR production rate, UCS uniaxial compressive strength, MH Mohs hardness, NPP predictor parameter

**Table 6** The values of PR, UCS and MH from the Almasi et al. (2017b) research and also their calculated values of NPP from Eq. (1) developed in this study

Commercial name	Scientific name	Rock class	PR (cm <sup>2</sup> /s)	UCS (MPa)	MH	NPP (MPa)
Sefid-Afshar granite	Granite	Igneous	2.0	147	6.03	886.41
Sefid-Nehbandan granite	Granite	Igneous	1.8	145	5.71	827.95
Ghermez-Zafreh granite	Andesite	Igneous	3.1	103	5.02	517.06
Borujerd granite	Granite	Igneous	2.2	128	5.86	750.08
Jade-Abrisham granite	Gabbro	Igneous	2.5	91	5.91	537.81
Morvarid-Mashhad granite	Granite	Igneous	2.3	113	5.62	635.06
Meshki-Natanz granite	Diorite	Igneous	1.5	147	6.12	899.64
Sabz-Piranshahr granite	Syenite	Igneous	1.8	193	5.83	1125.19
Sabz-Birjand granite	Diorite	Igneous	2.5	124	5.62	696.88
Sefid-Natanz granite	Granite	Igneous	2.9	105	5.11	536.55
Ghermez-Yazd granite	Andesite	Igneous	1.9	126	6.15	774.90

PR production rate, UCS uniaxial compressive strength, MH Mohs hardness, NPP predictor parameter

represented by the distance that each data point has from the 1:1 diagonal line. Since the points in Figs. 7, 8, and 9 are scattered uniformly around the diagonal line, it indicates that the proposed empirical equations are good models for prediction of PR of the samples under study. However, for the NPP, the data points fall closer to the diagonal line and are scattered lower than UCS and MH. These suggest that the ability to predict PR using the NPP test is more reliable than UCS and MH.

Consequently, comparison of determination coefficients, statistical analyses (t-test) of Eqs. 7–9 and scatter diagrams exhibited that the prediction performance of PR by NPP is better than those based on UCS and MH. Therefore, NPP is more appropriate and reliable than UCS and MH for prediction of PR of samples.

## Validity proposed parameter

The validity of NPP for prediction of PR in this study has been evaluated by using the raw data obtained from the experimental works of two researchers. Mikaeil et al. (2013b) used from UCS and MH for ranking the sawability of ornamental stone using Fuzzy Delphi and multi-criteria decision-making techniques. Almasi et al. (2017b) experimentally investigated the bead wear in diamond wire sawing considering the UCS, MH and PR for igneous rock. The measured values of PR, UCS and MH in Mikaeil et al. (2013b) and Almasi et al. (2017b) researches are summarized in Tables 5 and 6. The NPP proposed in this study (Eq. 1) was calculated for raw data obtained from these researchers. The NPP values are given in Tables 5 and 6. The derived NPP values in this study (Table 2) were compared with those available in the Mikaeil et al. (2013b) and the Almasi et al. (2017b) researches

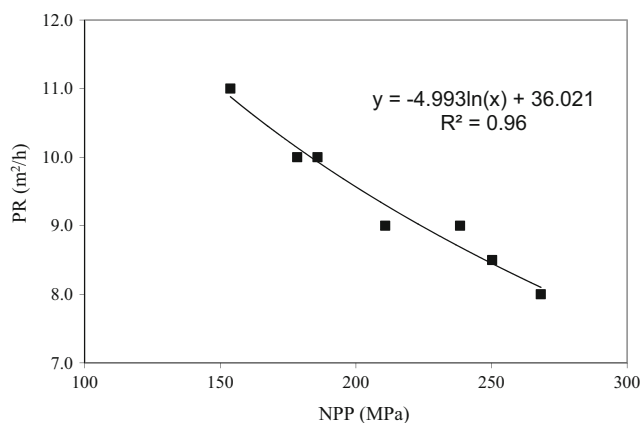


**Fig. 10** The correlation between PR and NPP for the Mikaeil et al. (2013b) research (Table 5)

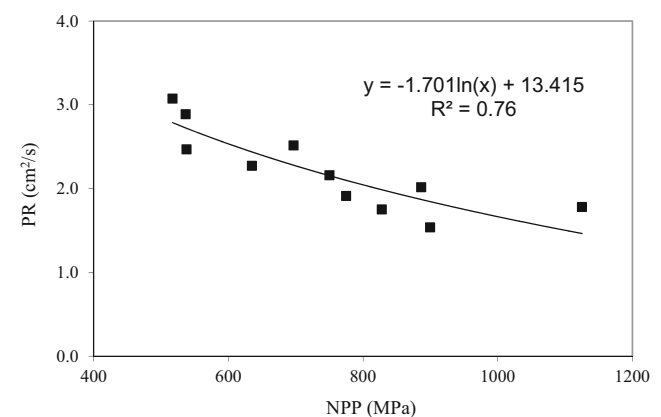


**Fig. 11** The correlation between PR and NPP for the Almasi et al. (2017b) research (Table 6)



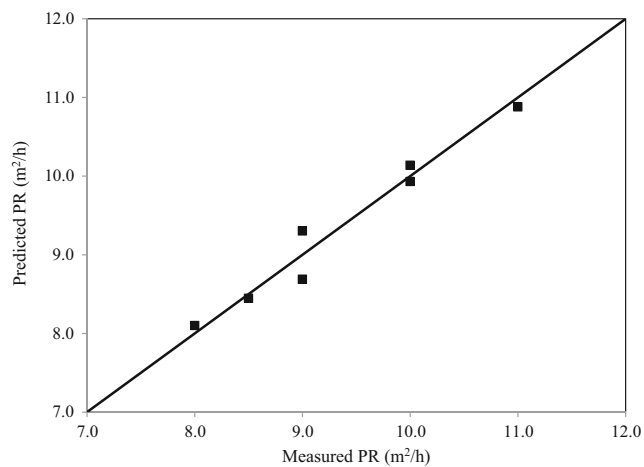


**Fig. 12** The measured PR by Mikaeil et al. (2013b) versus the predicted PR from Eq. (6)

(Tables 5 and 6). It is worth noting that there is a significant difference between the results of this study and Almasi et al. (2017b) with Mikaeil et al. (2013b). The NPP for hard igneous rocks in this study and Almasi et al. (2017b) varies from 431.48 to 1125.19; whereas those obtained by Mikaeil et al. (2013b) for carbonate rocks were ranging between 153.70 and 268.20. The difference in the NPP values is due to higher UCS and MH in igneous rocks when compared with limestone, which has caused a higher value of the NPP in them.

Then, correlations between PR and NPP were developed, and their determination coefficients were determined. Figures 10 and 11 show the relationship between PR and NPP for the Mikaeil et al. (2013b) and the Almasi et al. (2017b) researches, respectively. It can be seen from the figures that, in both cases, the best-fitted correlations were found to be represented by logarithmic regression curves. In Figs. 10 and 11, the trend of data shows a decrease in PR with the

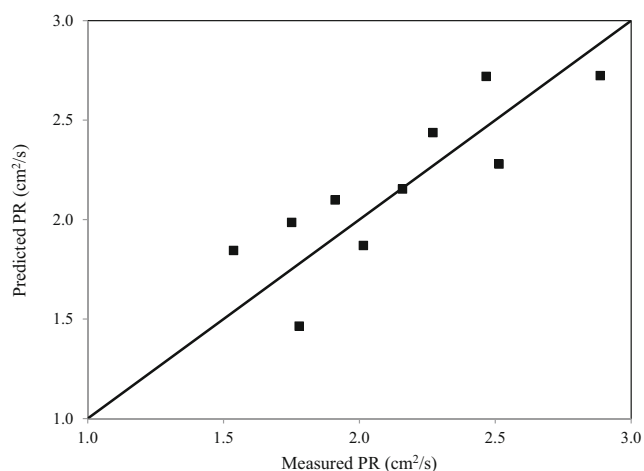


**Fig. 13** The measured PR by Almasi et al. (2017b) versus the predicted PR from Eq. (7)

increase in the NPP. Based on data given in Table 5, a very good logarithmic relationship was obtained between PR and NPP with the determination coefficient of 0.96 (Fig. 10). The equation for the relationship is:

$$PR = -4.993 \ln(NPP) + 36.021 \quad R^2 = 0.96 \quad (6)$$

According to data given in Table 6, similarly a logarithmic relationship was observed between PR with NPP with a lower determination coefficient using the equation (Fig. 11):

$$PR = -1.701 \ln(NPP) + 13.415 \quad R^2 = 0.76 \quad (7)$$

Although the determination coefficients of the Eqs. 6 and 7 are 0.96 and 0.76, respectively, and these are good values especially for Eq. 6, it does not validate the Eqs. necessarily. Therefore, for validating Eqs. 6 and 7, the predicted values were plotted against the measured values in Figs. 12 and 13.

Since the points in Figs. 12 and 13 are scattered uniformly around the diagonal line, it indicates that Eqs. 6 and 7 are good models. It can be concluded that NPP could be used as a parameter for prediction of the production rate in rock sawing.

## Conclusion

In this study, a simple predictor parameter (NPP) based on uniaxial compressive strength (UCS) and Mohs hardness (MH) was developed for prediction of production rate (PR) of ornamental stones. The validity of NPP was carried out by considering the *t*-test, the plots of predicted PR values versus the measured PR values, and also by using the raw data obtained from the experimental works of two researchers. The results indicated that the predictor parameter has good accuracy for prediction of PR, and thus making a rapid assessment of the sawability of ornamental stones. Consequently, the NPP developed in this study provides significant practical advantages for prediction of PR and saves much time and cost in during the quarry planning and design. However, this is valid for rocks produced from nearly the same regions and having nearly the same rock properties. To use NPP in other regions, it should be evaluated for the rocks under study. Then, the PR of the rocks is determined. Finally, the statistical equation is developed between PR and NPP using simple regression analysis for prediction of PR.

## References

- Almasi SN, Bagherpour R, Mikaeil R, Ozcelik Y, Kalhori H (2017a) Predicting the building stone cutting rate based on rock properties

- and device pullback amperage in quarries using M5P model tree. *Geotech Geol Eng* 35:1311–1326
- Almasi SN, Bagherpour R, Mikaeil R, Ozcelik Y (2017b) Analysis of bead wear in diamond wire sawing considering the rock properties and production rate. *Bull Eng Geol Environ*. <https://doi.org/10.1007/s10064-017-1057-9>
- Armaghani DJ, Mohamad ET, Hajihassani M, Yagiz S, Motaghedi H (2016) Application of several non-linear prediction tools for estimating uniaxial compressive strength of granitic rocks and comparison of their performances. *Eng Comput* 32:189–206
- Ataei M, Mikaeil R, Sereshki F, Ghaysari N (2012) Predicting the production rate of diamond wire saw using statistical analysis. *Arab J Geosci* 5:1289–1295
- Atici U, Ersoy A (2009) Correlation of specific energy of cutting saws and drilling bits with rock brittleness and destruction energy. *J Mater Process Technol* 209:2602–2612
- Aydin G, Karakurt I, Hamzacebi C (2015) Performance prediction of diamond sawblades using artificial neural network and regression analysis. *Arab J Sci Eng* 40:2003–2012
- Bagherpour R, Khademian A, Almasi SN, Aalaei M (2014) Optimum cutting wire assembly situation in dimension stone quarries. *J Min Metall Metall* 50:1–8
- Beiki M, Majidi A, Givshad AD (2013) Application of genetic programming to predict the uniaxial compressive strength and elastic modulus of carbonate rocks. *Int J Rock Mech Min Sci* 63:159–169
- Bianconi F, Gonzalez E, Fernandez A, Saetta SA (2012) Automatic classification of granite tiles through colour and texture features. *Expert Sys App* 39:11212–11218
- Burgess RB (1978) Circular sawing granite with diamond saw blades. In: *Proceedings of the fifth industrial diamond seminar*, 3–10
- Buyuksagis IS (2007) Effect of cutting mode on the sawability of granites using segmented circular diamond sawblade. *J Mater Process Technol* 183:399–406
- Ceryan N (2014) Application of support vector machines and relevance vector machines in predicting uniaxial compressive strength of volcanic rocks. *J Afr Earth Sci* 100:634–644
- Chatterjee TK, Chatterjee R, Singh S (2005) Classification of black decorative stones from Warangal District, Andhra Pradesh, India. *Bull Eng Geol Environ* 64:167–173
- Clausen R, Wang CY, Meding M (1996) Characteristics of acoustic emission during single diamond scratching of granite. *Ind Diam Rev* 3:96–99
- Delgado NS, Rodriguez R, Rio A, Sarria ID, Calleja L, Argandona VGR (2005) The influence of microhardness on the sawability of pink Porrino granite (Spain). *Int J Rock Mech Min Sci* 42:161–166
- Ersoy A, Atici U (2004) Performance characteristics of circular diamond saws in cutting different types of rocks. *Diam Relat Mater* 13:22–37
- Ersoy A, Buyuksagis IS, Atici U (2005) Wear characteristics of circular diamond saws in the cutting of different hard and abrasive rocks. *Wear* 258:1422–1436
- Eyuboglu AS, Ozcelik Y, Kulaksiz S, Engin IC (2003) Statistical and microscopic investigation of disc segment wear related to sawing Ankara andesites. *Int J Rock Mech Min Sci* 40:405–414
- Fener M, Kahraman S, Ozder MO (2007) Performance prediction of circular diamond saws from mechanical rock properties in cutting carbonate rocks. *Rock Mech Rock Eng* 40(5):505–517
- Ghaysari N, Ataei M, Sereshki F, Mikaeil R (2012) Prediction of performance of diamond wire saw with respect to texture characteristics of rock. *Arch of Min Sci* 57(4):887–900
- Gunaydin O, Kahraman S, Fener M (2004) Sawability prediction of carbonate rocks from brittleness indexes. *J South Afr Inst Min Metall* 104:239–244
- Guney A (2011) Performance prediction of large-diameter circular saws based on surface hardness tests for Mugla (Turkey) marbles. *Rock Mech Rock Eng* 44:357–366
- ISRM (1981) Rock characterization testing and monitoring. ISRM suggested methods. In: Brown ET (ed)
- ISRM (2007) The complete ISRM suggested methods for rock characterization, testing and monitoring. In: Ulusay R, Hudson JA (eds.), Suggested methods prepared by the commission on testing methods (1974–2006)
- Jamshidi A, Nikudel MR, Khamehchiyan M (2017) A novel physico-mechanical parameter for estimating the mechanical strength of traversines after a freeze-thaw test. *Bull Eng Geol Environ* 76(1):181–190
- Jennings M, Wright DN (1989) Guidelines for sawing stone. *Ind Diam Rev* 49:70–75
- Kahraman S, Fener M, Gunaydin O (2004) Predicting the sawability of carbonate rocks using multiple curvilinear regression analysis. *Int J Rock Mech Min Sci* 41(7):1123–1131
- Kahraman S, Altunb H, Tezekicib BS, Fener M (2006) Sawability prediction of carbonate rocks from shear strength parameters using artificial neural networks. *Int J Rock Mech Min Sci* 43:157–164
- Kainthola A, Singh P, Verma D, Singh R, Sarkar K, Singh T (2015) Prediction of strength parameters of Himalayan rocks: a statistical and ANFIS approach. *Geotech Geol Eng* 33:1255–1278
- Madhubabu N, Singh P, Kainthola A, Mahanta B, Tripathy A, Singh T (2016) Prediction of compressive strength and elastic modulus of carbonate rocks. *Meas* 88:202–213
- Mikaeil R, Ataei M, Hoseinie SH (2008) Predicting the production rate of diamond wire saws in carbonate rock cutting. *Ind Diam Rev* 3:28–34
- Mikaeil R, Ataei M, Yousefi R (2013a) Correlation of production rate of ornamental stone with rock brittleness indexes. *Arab J Geosci* 6(1): 115–121
- Mikaeil R, Ozcelik Y, Yousefi R, Ataei M, Hosseini SM (2013b) Ranking the sawability of ornamental stone using fuzzy Delphi and multi-criteria decision-making techniques. *Int. J. Rock Mech Min Sci* 58:118–126
- Mishra D, Basu A (2013) Estimation of uniaxial compressive strength of rock materials by index tests using regression analysis and fuzzy inference system. *Eng Geol* 160:54–68
- Mohamad ET, Armaghani DJ, Momeni E, Abad SVANK (2015) Prediction of the unconfined compressive strength of soft rocks: a PSO-based ANN approach. *Bull Eng Geol Environ* 74:745–757
- Monjezi M, Khoshalan HA, Razifard M (2012) A neuro-genetic network for predicting uniaxial compressive strength of rocks. *Geotech Geol Eng* 30:1053–1062
- Norling RG (1971) Mechanical properties and the composition of some Swedish natural stone types and their effect on cutting results. Presentation at the Conference on Diamond in the Construction and Stone Industry (In German)
- Ozcelik Y (2005) Effect of mineralogical and petrographical properties of marble on cutting by diamond wire. *CIM Bull* 98(1085):1–6
- Ozcelik Y (2007) The effect of marble textural characteristics on the sawing efficiency of diamond segmented frame saws. *Ind Diam Rev* 2:65–70
- Ozcelik Y, Polat E, Bayram F, Ay AM (2004) Investigation of the effects of textural properties on marble cutting with diamond wire. *Int J Rock Mech Min Sci* 41(3):228–234
- Sadegheslam G, Mikaeil R, Rooki R, Ghadernejad S, Ataei M (2013) Predicting the production rate of diamond wire saws using multiple nonlinear regression analysis. *Geos Eng* 16:275–285
- Singh P, Tripathy A, Kainthola A, Mahanta B, Singh V, Singh T (2017) Indirect estimation of compressive and shear strength from simple index tests. *Eng Comput* 33:1–11
- Tumac D (2015) Predicting the performance of large diameter circular saws based on Schmidt hammer and other properties for some Turkish carbonate rocks. *Int J Rock Mech Min Sci* 75:159–168
- Tumac D (2016) Artificial neural network application to predict the sawability performance of large diameter circular saws. *Meas* 80:12–20
- Wright DN, Cassapi VB (1985) Factors influencing stone sawability. *Ind Diam Rev* 2:84–87
- Yurdakul M, Gopalakrishnan K, Akdas H (2014) Prediction of specific cutting energy in natural stone cutting processes using the neuro-fuzzy methodology. *Int J Rock Mech Min Sci* 67:127–135